3rd URSI AT-AP-RASC, Gran Canaria, 29 May – 3 June 2022

Challenges of Global-Scale Ionospheric Tomography using GNSS: A brief overview

Fabricio S. Prol(1)
(1) Department of Navigation and Positioning, Finnish Geospatial Research Institute (FGI/NLS), Kirkkonummi, Finland

Abstract

This work provides a brief overview of the main challenges found by the author when developing a global ionospheric electron density estimation using tomography and Global Navigation Satellite System (GNSS) data.

1. Introduction

Although several achievements have been obtained when applying tomography at regional scale, very few works have been conducted for the development of techniques at global scale. To the knowledge of the author, Juan et al. [1], Hernández-Pajares et al. [2], She et al. [3], Cheng et al. [4] and Prol et al. [5], have addressed the problem. Figure 1, for instance, shows an example of the 3D electron density spatial fields obtained by the method developed in Prol et al. [5]. It provides a worldwide 3D overview of the state of the electron density dynamics, which is relevant to describe and monitor the Space Weather. Despite of the good accuracy of the obtained 3D representations, many challenges are remaining. Eight of the main challenges found by the author are related to the (I) validation of tomographic techniques; (II) background accuracy; (III) GNSS biases; (IV) data gaps over large regions; (V) limitations on the spatial and temporal resolutions; (VI) poor system geometry due the limited signal elevations; (VII) non-optimized constraints and; (VIII) difficulties on real time applications. In the present work, an overview of these eight challenges is provided.

2. Validation of Tomographic Techniques

Ionospheric tomography is mainly applied using total electron content (TEC) observations as input for solving the unknown electron density **x** of each voxel of a 3D grid. The system can be formulated as:

$$\mathbf{y} = \mathbf{A}\mathbf{x} + \varepsilon \qquad (1)$$

where **y** stands for the vector of TEC measurements, the matrix **A** is composed by the path length of each TEC measurement inside the voxels, and ε is the system and measurement noises. In principle, the inversion of TEC measurements into electron density values is obtained by an estimation technique, such as least squares and Kalman filters; however, the electron density estimation is not an easy task due to poor geometry of the TEC measurements.

Over the years, several optimization techniques have been developed to overcome the poor condition of the system. Most of the techniques have been developed by independent researchers, providing local improvements. A question that remains, however, is: which tomographic technique can better invert the TEC values into 3D electron density spatial fields?

To properly answer the question, a direct comparison between several techniques would be necessary. Due to the complexity of each method, this may require the best efforts of different researchers to share the source codes. Sharing source codes can be an actual problem due to the internal policies of each institute or space weather center. Therefore, a more straightforward way would be to validate the model results in a standardized way. In this case, it is crucial to set up scenarios where all the distinct techniques can be applied to the same input TEC data and validated against the same electron density dataset. In this regard, a joint working group has been created by the Global Geodetic Observing System (GGOS) and the International Association of Geodesy (IAG) with the main goal of validating 3D electron density models. As shown in https://ggos.org/about/org/fa/geodetic-space-weather-research/groups/jwg1-electron-density-modelling/, the main task is to have a cross-validation between distinct 3D methods. So far, six case scenarios have been created in a platform with input and output values that researchers can run and share their results. In future, the created database is expected to be an open platform.

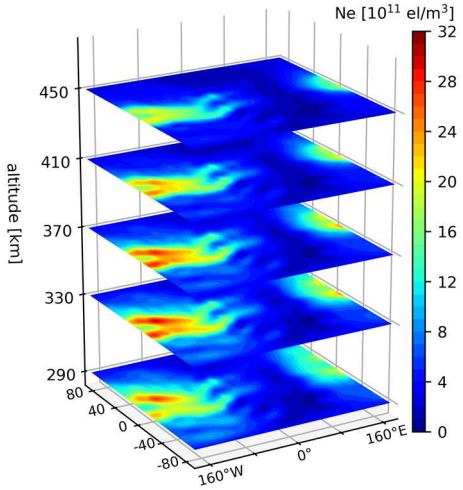

Figure 1. Electron density slices obtained by global tomography at 00 UT on the day of year 75 of 2015.

3. Background

The ionospheric background plays a crucial hole in the quality of the reconstructed electron density. As demonstrated by Prol et al. [6], an important requirement of tomography is the usage of a background that efficiently represents the profile shapes. This means that tomography has a great dependence on the background values such as the electron density scale height (Hs) and peak height (HmF2). Nowadays, it is very typical to use empirical models to define the background. Empirical models such as the International Reference Ionosphere (IRI) [7] and NeQuick [8] are being efficiently used in tomographic applications. Both models well describe the HmF2 and Hs values worldwide. However, at the specific instances of pre-reversal enhancement, underestimations at the Equatorial region are clearly observed by Prol et al. [9]. In such cases, it is expected worst estimations by tomography. A viable option to overcome this challenge, however, is the use of background models based on GNSS Radio-Occultation (RO) data, which have presented a good estimate of HmF2 during the pre-reversal enhancements [9]. A way to improve the global tomography is therefore by the incorporation of RO data into the background models, which may pose a challenge due to necessity of integration of the RO electron density measurements with other instruments, such as ionosondes, topside sounders, and in-situ Langmuir probes.

Another relevant point is that IRI provides electron density values from 60 to 2,000 km. This leads to a long path of the GNSS signal (2,000 to 20,000 km) without any initial guess. As a result, electron density overestimations are expected in tomography, as obtained in Prol et al. [10]. Alternatively, NeQuick allows the retrieval of the electron density up to 20,000 km; but clear underestimations of the electron density between 800 to 20,000 km are reported in recent works [11, 12, 13]. Therefore, a major challenge nowadays of the global tomography is the correct representation of the background plasmasphere. However, recent improvements in NeQuick [14] and topside representations [15, 16] suggest that new background specifications will overcome this problem in future.

4. GNSS Biases

When building a tomographic algorithm with GNSS observations, instrumental and/or ambiguity biases are required to be solved. In minimum, a daily bias term for each satellite and receiver must be included with the equation system. The challenge of this approach is that the data of several hours, or even for an entire day, need to be used for the bias estimation. In other words, several 3D grids (one for each time) and biases need to be solved in a single run. Since the equation system without biases is already ill-posed, the reconstructions become less stable as the spatial and temporal resolution are improved. A typical solution to the bias, therefore, is to pre-calibrate the GNSS data using a background [5], i.e., the bias term is estimated using the background model or Global Ionospheric Maps (GIMs). The problem of the pre-calibration is that the background and GIM inaccuracies are reflected in the TEC calibration, however, so far, the global-scale tomography techniques with high resolutions have mainly used pre-calibrated data. Another solution is representing the ionosphere with two or three layers [1, 2]; however, the reconstructions will be limited to represent very broad vertical information.

5. Data Gaps

GNSS data can provide considerably dense distribution of ionospheric points over the land surface. Open GNSS data initiatives, such as the provided by the international GNSS service (IGS) and regional networks all over the world, have extensively contributed to the possibility of a global tomography over the land surface. Based on 2700 GNSS ground-stations, Prol et al. [5] for instance, showed that accurate global reconstructions can be obtained at several places over the land. However, a challenge that remains is still due to data gaps over Africa, Asia, and Oceans (Figure 2). Perhaps, a future solution for regions with sparse GNSS stations is a collaborative platform of smartphones sharing GNSS data since a few studies are showing promising results with smartphone TEC data [17]. The limited data coverage in the ocean, however, cannot be so benefited by the smartphones. In this regard, GNSS data collected by moving ships or vessels offer an invaluable data source, such as presented in Hernández-Pajares et al. [18].

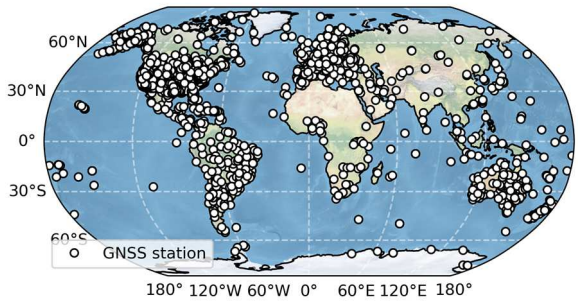

Figure 2. GNSS receivers location with open data access.

6. Spatial and Temporal Resolutions

According to the authors' knowledge, the highest resolution of global tomography to date [5] is 2° × 2° × 20 km for latitude, longitude, and altitude respectively, covering from 50 to 20,000 km in altitude with a temporal resolution of 15 min. Although this resolution was sufficient to capture main patterns of the ionosphere as well as signatures and disturbances of geomagnetic storm, this resolution may not be enough to capture finer ionospheric perturbation structures, such as plasma bubbles, medium- and low-scale traveling ionospheric disturbances (TIDs), and earthquake-induced disturbances. There is a great challenge on the usage of higher resolutions due to the number of unknowns in the imaging system. However, the computational power is rapidly evolving, and future developments will probably overcome the resolution challenge.

7. System Geometry

Nowadays, the ground-based GNSS measurements are the main source of TEC data. However, due to the almost vertical GNSS geometry of the ground-based observations, they only provide a limited number of viewing angles. The solution of equation (1) is therefore ill-conditioned when using several ionospheric layers. Improvements on the system geometry can be achieved by the incorporation of TEC data observed by Low Earth Orbit (LEO) satellites. Although the number of LEO satellites has been sparse in the last decades, containing very few satellites at specific time instances, efforts have been conducted to the use of such instruments to cover the geometry gaps [4]. In high temporal resolutions, however, the number of LEO-based TEC measurements is rather limited nowadays. In this regard, efforts from the Formosa Satellite-7/Constellation Observing System for Meteorology Ionosphere and Climate, which recently launched six LEO satellites, and by the Spire Global Inc., continuously increasing the number of LEO satellites, will benefit the future system geometry of the global-scale tomography. In addition to the well-known RO satellites, new navigation systems based only on LEO satellites are planned to be materialized with dense constellations. In such cases, the global-scale tomography would be immensely benefited, as shown by Ren et al. [19]. The materialization of several LEO satellites with distinct altitudes will enlarge the signal viewing angles between the ground and LEO satellite as well as between the LEO and the GNSS satellites. Moreover, the navigation LEO constellations create a great opportunity of inter-link measurements between the LEO satellites, improving the system geometry considerably.

8. Optimized Constraints

First ionospheric tomography applications were based on regional reconstructions using the algebraic reconstruction technique (ART) [20]. In principle, ART provides fast updates of the ionosphere without applying constraints on the estimation, which poses a problem due to the poor system geometry. Later, some studies have shown that constrained techniques can improve the overall specification of the ionospheric tomography, e.g. [21]; however, the constraint dependence adds to the computational burden due to the additional matrix multiplications. In addition to the computational burden, some constrained techniques require a large data set with many intersections of the GNSS signals. Therefore, on a global scale, the large number of unknowns together with several data gaps precludes the possibility of using the most sophisticated constrained techniques [22]. To gain computational efficiency and make possible to solve the global tomography, optimized constrains, such as the proposed by Prol et al. [23], are a viable option to the global reconstructions since it does not incorporate a set of new matrix multiplications and, consequently, no relevant additional computational efforts. The drawback of this technique, however, is the high dependence on the shape of the profiles provided by the background. So, no relevant updates on the HmF2 are expected. Therefore, new studies are required to focus on the development of system constraints which are viable to be used at global scale.

9. Real Time

At global-scale, the large number of unknowns, together with the excessive number of GNSS stations, poses high demands to the computational burden. Due to this reason, fast inversion techniques, such as ART, are being efficiently used to solve equation (1). In the most recent works, Prol et al. [5] completed the computation of a single snapshot of the electron density distribution within 20 to 30 min. Even faster, Cheng et al. [4] achieved 10 min computation time, despite using less GNSS stations. Therefore, the global-scale tomography is already not so far from real-time. A main point in the future is the usage of better parallel computing tools, which can reduce the computational time. However, we would still be in near real time in the best-case scenario. The real-time challenge could be better solved with the development of prediction techniques of the electron density distributions. In the prediction scenario, the integration of tomography with physics-based models on a genuine data assimilation scheme seems to be the most straightforward step. However, this integration may include additional errors due to the dependence of tomography on the internal accuracy of the physics model.

10. Final Remarks

The overall capabilities of ionospheric tomography at global-scale are evident in Prol et al. [5]. However, many challenges are compromising the estimations. As reported in the present work, advances are still needed in the cross validation between distinct tomography techniques, improvements on empirical models, computational capabilities, data coverage and system geometry. Despite all the challenges, a bright future is expected since upcoming improvements are expected in the validation techniques, background specifications, computational power, GNSS technologies, and satellite constellations.

11. Acknowledgements

This work is funded by the INdoor navigation from CUBesAT Technology project, under the grant from the Technology Industries of Finland Centennial Foundation and Jane and Aatos Erkko Foundation.

References

[1] J. M. Juan, A. Rius, M. Hernández-Pajares, and J. Sanz, “A two-layer model of the ionosphere using global positioning system data,” *Geophys. Res. Lett.*, **24**, 1997, pp. 393–396, doi: 10.1029/97GL00092

[2] M. Hernández-Pajares, J. M. Juan, J. Sanz, and J. G. Solé, “Global observation of the ionospheric

electronic response to solar events using ground and LEO GPS data," *J. Geophys. Res.*, **103**, 1998, pp. 20789-20796, doi: 10.1029/98JA01272

[3] C. She, W. Wan, X. Yue, B. Xiong, Y. Yu, F. Ding, and B. Zhao, "Global ionospheric electron density estimation based on multisource TEC data assimilation," *GPS Solut.*, **21**, 2017, pp. 1125-1137, doi:10.1007/s10291-016-0580-7

[4] N. Cheng, S. Song, G. Jiao, X. Jin, and W. Li, "Global monitoring of geomagnetic storm-induced ionosphere anomalies using 3-D ionospheric modeling with multi-GNSS and COSMIC measurements," *Radio Sci.*, **56**, 2021, pp. e2020RS007074, doi: 10.1029/2020RS007074

[5] F. S. Prol, T. Kodikara, M. M. Hoque, and C. Borries, "Global-scale ionospheric tomography during the March 17, 2015 geomagnetic storm," *Space Weather*, **19**, 2021, pp. e2021SW002889, doi: 10.1029/2021SW002889

[6] F. S. Prol, P. O. Camargo, and M. T. A. H. Muella, "Numerical simulations to assess ART and MART performance for ionospheric tomography of Chapman profiles," *An Acad Bras Cienc.*, **89**, 2017, pp. 1531-1542, doi: 10.1590/0001-3765201720170116

[7] D. Bilitza, D. Altadill, V. Truhlik, V. Shubin, I. Galkin, B. Reinisch, and Huang, X, "International Reference Ionosphere 2016: From ionospheric climate to real-time weather predictions," *Space Weather*, **15**, 2017, pp. 418-429, doi: 10.1002/2016SW001593.

[8] B. Nava, P. Coisson, S. M. Radicella, "A new version of the NeQuick ionosphere electron density model," *J. Atmos. Sol.-Terr. Phys.*, **70**, 2008, pp. 1856-1862, doi:10.1016/j.jastp.2008.01.015

[9] F. S. Prol, P. O. Camargo, M. Hernández-Pajares, and M. T. A. H. Muella, "A new method for ionospheric tomography and its assessment by ionosonde electron density, GPS TEC, and single-frequency PPP," *IEEE Trans. Geosci. Remote Sens.*, **57**, 2019, pp. 2571–2582, doi: 10.1109/TGRS.2018.2874974

[10] F.S. Prol, P.O. Camargo, "Ionospheric tomography using GNSS: multiplicative algebraic reconstruction technique applied to the area of Brazil," *GPS Solut.*, **20**, 2016, pp. 807-814, doi:10.1007/s10291-015-0490-0

[11] F.S. Prol, and M. M. Hoque, "Topside Ionosphere and Plasmasphere Modelling Using GNSS Radio Occultation and POD Data," *Remote Sens.*, **13**, 2021, pp. 1559, doi:10.3390/rs13081559

[12] A. Kashcheyev, and B. Nava, "Validation of NeQuick 2 model topside ionosphere and plasmasphere electron content using COSMIC POD TEC," *J. Geophys. Res. Space Phys.*, **124**, 2019, pp. 9525-9536, doi: 10.1029/2019JA026971

[13] M. M. Hoque, N. Jakowski, and F. S. Prol, "A new climatological electron density model for supporting space weather services," *J. Space Weather Space Clim.*, Accepted article, doi:10.1051/swsc/2021044

[14] M. Pezzopane, A. Pignalberi, "The ESA Swarm mission to help ionospheric modeling: A new NeQuick topside formulation for mid-latitude regions," *Sci. Rep.*, **9**, 2019, pp. 12253, doi: 10.1038/s41598-019-48440-6

[15] F.S. Prol, M. Hernández-Pajares, P. O. Camargo, and M.T.A.H. Muella, "Spatial and temporal features of the topside ionospheric electron density by a new model based on GPS radio occultation data," *J. Geophys. Res. Space Phys.*, **123**, 2018, pp. 2104–2115, doi:10.1002/2017JA024936

[16] F. S. Prol, D. R. Themens, M. Hernández-Pajares, P. O. Camargo, M. T. A. H. Muella, "Linear Vary-Chap Topside Electron Density Model with Topside Sounder and Radio-Occultation Data," *Surv. Geophys.*, **40**, 2019, 277-293, doi:10.1007/s10712-019-09521-3

[17] J. Bruno, F. Darugna, K. Bolmgren, J. B. Wübbena, C. Mitchell, M. Schmitz, "Quality analysis of dual-frequency smartphone-based ionospheric TEC measurements: what can be achieved?," *Ann. Geophys.*, **64**, 2021, pp. RS103, doi:10.4401/ag-8517

[18] M. Hernández-Pajares, H. Lyu, M. Garcia-Fernandez, and R. Orus-Perez, "A new way of improving global ionospheric maps by ionospheric tomography: Consistent combination of multi-GNSS and multi-space geodetic dual-frequency measurements gathered from vessel-, LEO- and ground-based receivers," *J. Geod.*, **94**, 2020, pp. 73, doi: 10.1007/s00190-020-01397-1

[19] X.Ren, D. Mei, X. Zhang, M. Freeshah, and S. Xiong, "Electron density reconstruction by ionospheric tomography from the combination of GNSS and upcoming LEO constellations," *J. Geophys. Res. Space Phys.*, **126**, 2021, pp. e2020JA029074, doi:10.1029/2020JA029074

[20] J. R. Austen, S. J. Franke, and C. H. Liu, "Ionospheric imaging using computerized tomography," *Radio Sci.*, **23**, 1988, pp. 299–307. doi:10.1029/RS023i003p00299

[21] Y. Yao, C. Zhai, J. Kong, C. Zhao, Y. Luo, and L. Liu, "An improved constrained simultaneous iterative reconstruction technique for ionospheric tomography, *GPS Solut.*, **24**, 2020, pp. 68, doi: 10.1007/s10291-020-00981-4

[22] G. K. Seemala, M. Yamamoto, A. Saito, and C. H. Chen, "Three-dimensional GPS ionospheric tomography over Japan using constrained least squares," *J. Geophys. Res. Space Phys.*, **119**, 2014, pp. 3044-3052, doi: 10.1002/2013JA019582

[23] F. S. Prol, M. M. Hoque, and A. A. Ferreira, "Plasmasphere and topside ionosphere reconstruction using METOP satellite data during geomagnetic storms," *J. Space Weather Space Clim*, **11**, 2021, pp. 5, doi:10.1051/swsc/2020076